J. Biochem. **127**, 1095–1102 (2000)

The Effect of Single Residue Substitutions of Serine-283 on the Strength of Head-to-Tail Interaction and Actin Binding Properties of Rabbit Skeletal Muscle α-Tropomyosin[1]

Ken-Ichi Sano,[2] Kayo Maeda,[2] Toshiro Oda,[3] and Yuichiro Maéda[2,4]

International Institute for Advanced Research, Central Research Laboratories, Matsushita Electric Industrial, Hikari-dai, Seika, Kyoto 619-0237

Received January 25, 2000; accepted March 30, 2000

Vertebrate skeletal muscle α-tropomyosin polymerizes in a head-to-tail manner and binds cooperatively to actin. It has been postulated that the cooperative actin binding is governed by the strength of the head-to-tail interaction. In order to know the relationship between the head-to-tail affinity and actin binding, we studied the properties of tropomyosin variants with single residue substitutions at serine-283, the penultimate residue at the carboxyl terminus that is involved in the head-to-tail interaction. It has been shown that the phosphorylation of serine-283 strengthens the head-to-tail interaction. Viscometry was employed to compare the head-to-tail affinity of tropomyosin variants. Variant S283E showed higher viscosity whereas variant S283K showed lower viscosity compared with the wild type non-phosphorylated α-tropomyosin. The results confirm the idea that the interaction is sensitive to the ionic properties of residue 283. The strength of the head-to-tail interaction was assessed directly by sedimentation equilibrium using two pairs of tropomyosin variants designed so that only dimeric interactions were allowed within each pair. From one pair of variants with serine-283, the association constant was determined to be 2.6×10^4 M^{-1} (SD = 1.0×10^4), whereas for the second pair with glutamate-283, the affinity was 3.9×10^4 M^{-1} (SD = 1.6×10^4), slightly stronger than the former, consistent with the results of viscometry. The results indicate that the head-to-tail association is weak as previously implicated from light scattering measurements. Cosedimentation was employed to measure the cooperative actin binding of tropomyosin variants. Although previous results indicated the phosphorylation has no significant influence on the actin affinity, variant S283E shows a lower affinity compared with the control. Variants S283K and S283A show even lower affinities to actin, although these species bind to actin more cooperatively than does variant S283E. The results indicate that the affinity of the head-to-tail interaction between adjacent tropomyosin molecules is weak, and is substantially influenced by an extra charge at residue 283. On the other hand, the interaction with actin, the affinity and the cooperativity in actin binding, is dependent on amino acid residues at 283 and is not simply correlated with the strength of the head-to-tail interaction between Tm molecules in solution.

Key words: α-helical coiled-coil, muscle thin filament, phosphorylation, polymerization, tropomyosin.

In vertebrate skeletal and cardiac muscles, Tropomyosin (Tm) in association with troponin plays a central role in the calcium regulation of muscle contraction (*1*). Tropomyosin is a highly anisotropic rod-like protein, 400 Å long and 20 Å thick, consisting of an α-helical coiled-coil spanning over almost the entire length of the molecule. The molecule consists of two identical (αα-) or near-identical (αβ-) polypeptide chains, each consisting of 284 amino acids with a molecular mass of about 33 kDa, aligned in parallel and in register (*2, 3*). We denote αα-Tm as α-Tm in this text. It is now well known that tropomyosin isoforms are widely distributed in non-muscle cells, where they are always associated

[1] This work was supported in part by Special Coordination Funds for Promoting Science and Technology of the Science and Technology Agency of the Japanese Government.

Present addresses: [2] Laboratory for Structural Biochemistry, RIKEN Harima Institute at SPring-8, Kouto, Mikazuki, Sayo, Hyogo 679-5148; [3] Department of Biophysics, Max Planck Institute for Medical Research, Jahnstrasse 29, D-69120 Heidelberg, Germany, on leave from RIKEN Harima Institute at SPring-8.

[4] To whom correspondence should be addressed. Phone: +81-791-58-2822, Fax: +81-791-58-2836, E-mail: ymaeda@spring8.or.jp

Abbreviations: Tm, tropomyosin; bvTm, tropomyosin expressed using a baculovirus based expression system in Sf9 cultured insect cells; F-actin, filamentous actin; PCR, polymerase chain reaction; Sf9, *Spodoptera frugiperda* insect cell; Tris, tris-(hydroxymethyl)-amino-methane; DTT, dithiothreitol; EDTA, ethylene-diamine-tetra-acetic acid; HEPES, 2-[4-(2-hydroxyethyl)-1-piperazinyl]-ethane-sulfonic acid; SDS, sodium dodecyl sulfate; PAGE, polyacrylamide gel electrophoresis.

with actin and presumably make actin filaments more stable (*4*).

At low ionic strengths, tropomyosin polymerizes (*5*) through interactions to form head-to-tail linear aggregates, presumably through the overlap of 8–9 residues between the N- and the C-termini of two adjacent Tm molecules (*6*). It is believed that this head-to-tail interaction also exists in the muscle thin filament where tropomyosin strands lie along the grooves of polymerized actin (*7*). The binding isotherms of tropomyosin to actin are sigmoidal, indicating the cooperative binding of Tm. The cooperative binding has been attributed to the head-to-tail interaction between Tm's that are bound contiguously along the actin filaments (*8–10*). This implies that Tm species with stronger head-to-tail interactions will show higher cooperativity in actin binding. The present study was designed to address the question of how the head-to-tail affinity and actin-binding properties correlate with one another.

Since the structure of the termini of Tm molecules are likely to be involved in both the actin binding and head-to-tail interaction, it is possible that the manner of the head-to-tail interaction affects the manner of actin binding. In the present study, we investigated the possible correlation between the two by using variants of α-Tm in which serine-283, the penultimate residue at the C-terminus, is replaced by another amino acid to alter the strength of the head-to-tail interaction. This residue is the unique phosphorylation site of skeletal muscle α-Tm (*11*), and phosphorylation of this residue increases the propensity for head-to-tail interaction (*12*), although the physiological roles of this phosphorylation are not known.

Previous studies have indicated that the head-to-tail interaction is not a prerequisite for actin binding. Removal of 11 residues from the C-terminus by proteolysis results in the loss of both polymerizability and actin affinity. However, close inspection of the time course of proteolysis shows that the loss of polymerizability does not occur concomitantly with the loss of actin affinity (*13*). *Escherichia coli* express skeletal muscle α-Tm that has an unacetylated N-terminus, another type of terminal defect, and is not polymerizable or able to bind actin (*14*). On the other hand, Tm isoforms with the smooth muscle type C-terminal sequence (*15*, *16*) as well as some non-muscle isoforms (*17*), do not polymerize effectively but do bind cooperatively to F-actin.

In the present study, the strength of the head-to-tail interaction was measured not only by viscometry but also by sedimentation equilibrium. Although the viscosity is easy to measure and provides a good measure of the strength of the head-to-tail interaction, the absolute value of viscosity is difficult to interpret. Moreover, the viscosity is also influenced by many other factors, especially by side-by-side interactions between molecules, and this is not negligible for Tm (*18*). On the other hand, sedimentation equilibrium, an ideal method for determining the association constant between two species of molecules, can not be employed in a straight-forward fashion to linear aggregates of heterogeneous length distribution. Therefore, in the present study, two types of Tm variants were prepared, one with an intact N- and a defective C-terminus and the other with a defective N- and an intact C-terminus, so that the molecular interaction was restricted to dimerization between the pair of variants.

The results indicate that the strength of the head-to-tail interaction is weak and affected by the electric charge of residue 283, and that neither the affinity nor the cooperativity of actin binding of α-Tm is in direct proportion to the strength of the head-to-tail interaction, which is measured between adjacent Tm molecules not interacting with actin.

MATERIALS AND METHODS

Construction of the Tropomyosin Transfer Vectors and Tropomyosin Expression Vectors—The cDNA cloning, DNA sequencing and expression of rabbit wild type skeletal α-Tm have already been described (*19*). The oligonucleotides shown in Table I were designed on the basis of the previously reported Tm sequence (*19*).

Expression vectors for Tm Δ1-140 and Tm Δ1-140 S283E were constructed by PCR. The sequence of the PCR primers were designed so that the PCR products had a *Nco*I site at the initiation codon and a *Bam*HI site after the termination codon. PCR products were digested with both *Nco*I and *Bam*HI. The fragments were ligated with expression vector pET3d (*20*) which was digested by both *Nco*I and *Bam*HI.

Construction of the transfer vector for Tm Δ274-284 was performed by single stranded site directed mutagenesis. The mutagenesis was carried out using the Tm gene subcloned into M13mp18 as a template DNA as described previously (*19*) according to the protocol provided by the supplier (Sculptor™ *in vitro* mutagenesis system, Amersham). The prepared double stranded DNA fragments were ligated into transfer vector pAcC4 (*21*) which was digested with *Nco*I and *Bam*HI.

Transfer vectors for Tm S283A, Tm S283E, and Tm S283K were constructed as follows. An *Mlu*I site was introduced at the C-terminal region of the Tm sequence by sin-

TABLE I. **List of mutants and primers for mutagenesis.**

Name	Mutation site	Mutation primers	Vector	Host cell	Yield (mg/liter)
bvTm			pAcC4	Sf9	6–10
Tm S283A	Ser283→Ala	5′- cgcg ct caac gat at gact gcc at at ag-3′ 3′ - gagt tgct at act gacggt at at cct ag-5′	pAcC4	Sf9	6–10
Tm S283E	Ser283→Glu	5′- cgcg ct caac gat at gact gag at at ag-3′ 3′ - gagt tgct at act gact ct at at cct ag-5′	pAcC4	Sf9	6–10
Tm S283K	Ser283→Lys	5′- cgcg ct caac gat at gact aag at at ag-3′ 3′ - gagt tgct at act gatt ct at at cct ag-5′	pAcC4	Sf9	6–10
TmΔ274-284	Leu274→amber	5′- agagcgt ggt cct act cct cgct gat-3′	pAcC4	Sf9	25–50
TmΔ1-140	Met141→initiate	5′- gat gaggaaacc at ggaaatt cag-3′ 5′- ct cgggat ccgt gaagcaaagaaac-3′	pET3d	*E. coli* BL21 (DE3)	20–30
TmΔ1-140 S283E	Met141→initiate Ser283→Glu	5′- gat gaggaaacc at ggaaatt cag-3′ 5′- ct agaggat cct at at ct cagt c - 3′	pET3d	*E. coli* BL21 (DE3)	20–30

gle stranded site-directed mutagenesis as described above. The isolated *Nco*I–*Mlu*I fragments of Tms were ligated to the annealed oligonucleotides containing an altered C-terminal sequence and *Mlu*I or *Bam*HI cohesive sequences at each end, as well as to pAcC4 digested by *Nco*I and *Bam*HI.

The sequences of the Tm variants in Table I were confirmed by DNA sequencing. Other procedures for DNA manipulation were performed according to (*22*).

Expression of Tropomyosin Variants in Insect Cells—The procedures employed have already been described elsewhere (*23*).

Expression of Tropomyosin Variants in Escherichia coli—The procedures already published (*19*) were employed with some modifications. The expression vectors were transformed into *E. coli* BL21 (DE3) strain, and bacterial cells were cultured in LB medium with 50 μg/ml ampicillin at 37°C. Induction was carried out at OD_{600} 0.8–0.9 by adding IPTG at a final concentration of 0.3 mM. The cells were harvested 3 hours after induction by centrifugation at 3,600 ×*g* for 10 min, washed with 50 mM Tris-HCl pH 8.0 and 1 mM EDTA, and stored frozen at –80°C.

Purification of Expressed Tropomyosin Variants—All the tropomyosin variants used in the present study were purified by the same procedures, although some variants are much shorter in molecular length than the others. Procedures already described elsewhere (*19*, *23*) were employed with an extra purification step at the end. After purification on a Mono-Q column, the Tm fractions were dialyzed against 100 mM potassium-phosphate buffer, pH 6.8, 300 mM KCl and 0.5 mM DTT, and applied to a hydroxyapatite column (Gigapito, Seikagaku Corporation), from which the Tms were eluted with a 400 ml gradient of 100–500 mM potassium phosphate buffer. Before the experiments, the Tms were denatured in 4 M guanidine hydrochloride and renatured by dialysis at 4°C against appropriate solutions for each experiment.

Purification of Rabbit Muscle Proteins—Actin was purified from the acetone powder of striated muscle of New Zealand White rabbits according to (*24*). Tm was purified from white skeletal muscle of rabbits according to (*25*) as a mixture of αα- and αβ-Tm. Purified Tm was dialyzed against 100 mM Tris-HCl, pH 8.0, 1 mM $MgSO_4$, and 1 mM DTT. One hundred units of bacterial alkaline phosphatase C75 (Nippon Gene) was added to the dialyzed Tm solution and the mixture was incubated for 4 h at 37°C. After the reaction, the solution was applied to the Mono-Q column described above to remove the bacterial alkaline phosphatase. The degree of dephosphorylation was checked by mass spectrometry as previously described (*26*).

Viscosity Measurements—Experiments were carried out at 25°C in an Ostowald type capillary viscometer for a sample volume of 1 ml. The flow rate of the buffer alone was 42 s. For measurements, the Tms were dialyzed against 10 mM Tris-HCl, pH 8.0, 10 mM KCl, and 0.5 mM DTT. The salt concentration was varied by adding small volumes of concentrated KCl solution to the Tm samples.

Circular Dichroism—Circular dichroism spectra were measured with a JASCO model J-720 spectropolarimeter using a cell with a 2 mm path length. Ellipticity values at 222 nm vs temperature were obtained automatically in 1°C steps after an equilibration time of 1 min and a data averaging time of 1 s. For each specimen, the temperature dependence was followed during both heating up and cooling down. The two curves were superimposed within experimental error. The solution conditions were either 5 μM (for TmΔ274-284) or 10 μM (for TmΔ1-140 and TmΔ1-140 S283E) of a Tm variant in 20 mM potassium phosphate buffer, pH 7.0, and 0.5 mM DTT.

Analytical Ultracentrifugation Analysis—Mixtures of 10–25 μM N-terminal truncated Tm (TmΔ1-140 or TmΔ1-140 S283E) and 5–20 μM C-terminal truncated Tm (TmΔ274-284) in a solution containing 20 mM potassium phosphate buffer, pH 7.0, and 0.5 mM DTT were loaded into Epon charcoal-filled standard sector cells, and placed in an An-60 Ti rotor. Centrifugation was performed in a Beckman Optima XL-A analytical ultracentrifuge at 8,000, 10,000, and 12,000 rpm at 20°C. The concentration gradient of the protein in the cell was determined by the average of four UV absorption measurements at 275 nm.

The sedimentation data were analyzed using an ideal heterogeneously associating model of the form A + B ↔ AB (*27*). The absorbance A_r at any radial r was fitted to the following equation.

$$A_r = \sum_{i=1}^{3} A_{i,r0} \exp\left(\frac{M_i(1-\rho v_i)\omega^2}{2RT}(r^2 - r_0^2)\right) \quad (1)$$

where suffix i represents a kind of species; 1 denotes an N-terminal truncated Tm; 2, a C-terminal truncated Tm; 3, a complex of an N-terminal truncated and a C-terminal truncated Tm. $A_{i,r}$ is the absorbance of the species i at a radial reference distance r_0 (=6.9 cm); ω the angular velocity; R, the gas constant; T, the Kelvin temperature; v_i, the partial specific volumes of species i; ρ, the solution density (=1.00 g/ml); M_i, the molecular weight of species i, which is 33,476 for TmΔ1-140, 33,560 for TmΔ1-140 S283E, and 63,038 for TmΔ274-284. The v_i, for each species was assumed to be 0.74 (ml/g), the value obtained from full-length Tm (*28*). The data were fitted to Eq. 1 using the Levenberg-Marquart Method using the routine in Origin™ version 4.0 (Microcal) with the constraint that the total optical density after integration over the cell depth should not exceed that of the protein loaded into the cell. The association constant is represented as

$$K_a = \frac{\varepsilon_1 M_1 \varepsilon_2 M_2}{\varepsilon_3 M_3} \frac{A_{3,r0}}{A_{1,r0} A_{2,r0}} \quad (2)$$

where ε_i is the weight absorption coefficient of species i in the centrifuge cell (absorbance values determined by centrifugation were checked using KNO_3 standard solution): 0.306 $(mg/ml)^{-1}$ for TmΔ274-284, 0.419 $(mg/ml)^{-1}$ for TmΔ1-140, and TmΔ1-140 S283E. The data sets were rejected, which indicates a clear tendency in the plot of the residual absorbance (the difference between fitted curve and the observed value) versus radius.

Actin-Binding Assay—Co-sedimentation combined with densitometry of the stained gels was employed. A mixture of 21 μM actin and 0.2–8 μM Tm was incubated at room temperature for 1.5 h in 70 μl of 13 mM HEPES-NaOH, pH 7.0, 60 mM NaCl, 3 mM $MgCl_2$, 0.5 mM DTT, and 1 mM NaN_3. After centrifugation at 70,000 rpm for 30 min at 20°C in a Beckman TL-100 centrifuge using a TLA 100 rotor, the supernatant and the pellet were separately subjected to SDS-PAGE in 12% acrylamide gels. The gels were stained with 0.1% Fast Green, and the resulting gel patterns were digitized by an image scanner (GT-8000, Epson),

and transferred to a Macintosh computer for further analysis using NIH-Image version 1.59. The amounts of Tm and actin in the gels were determined by comparing the integrated optical densities against standards obtained from known amounts of bvTm and actin. The apparent binding constants (K_{app}) and Hill coefficients (α_H) were determined using curve fitting routines within Origin™ (MicroCal) to fit the data points to the following equation:

$$v = n[\mathrm{Tm}]^{\alpha_H}K_{app}^{\alpha_H}/1 + [\mathrm{Tm}]^{\alpha_H}K_{app}^{\alpha_H}.$$

RESULTS

Expression of Tropomyosin Variants—The α-Tm variants used in the present study are indicated in Table I. When expressed in Sf9 cells, but not expressed in *E. coli*, the α-Tm molecule has an acetylated N-terminus like authentic Tm, and N-terminal acetylation is essential for its function (*19*, *29*). Therefore, all the variants that include the original N-terminus were expressed in Sf9 cells, including the wild type (bvTm), the full length variants with a single replacement at 283, and the variant with C-terminal truncation (TmΔ274-284). The N-terminal acetylation of some of these variants was confirmed by electron-spray mass spectrometry (data not shown). The yields of purified full length variants and TmΔ274-284 were 6–10 and 30–50 mg per liter of Sf9 cell culture, respectively. Two variants that include the C-terminal half were expressed in *E. coli* because N-terminal acetylation is not required. For these two, the yield was about 20 mg per liter of *E. coli* culture.

Viscosity Measurements of Tm Variants—In muscle, the penultimate serine-283 residue is partially phosphorylated (*11*). *In vitro*, the phosphorylation of serine-283 increases the viscosity of tropomyosin solutions at low ionic strengths, indicative of stronger head-to-tail interactions between molecules (*12*). This effect of phosphorylation is likely due to the extra negative charge associated with the phosphate group. Therefore, in order to alter the strength of the head-to-tail interaction, we replaced serine-283 with residues to alter the charge. To evaluate the strength of the head-to-tail interaction, the relative viscosities of these α-Tm variants were measured (*5*). Figure 1A shows the effect of ionic strength on viscosity at a fixed protein concentration. KCl concentration was altered from 10 to 100 mM. Figure 1B shows the effect of protein concentration from 25 μg/ml to 1 mg/ml on the viscosity at a fixed ionic strength. At all ionic strengths and protein concentrations tested, species with an uncharged amino acid residue at position 283, including the wild type α-Tm (bvTm), dephosphorylated authentic Tm (a mixture of αα-Tm and αβ-Tm) and Tm S283A, showed almost identical viscosities. With an extra negative charge at 283, Tm S283E showed a higher viscosity, while with an extra positive charge, Tm S283K showed a lower viscosity compared to the control (bvTm). These results confirm the suggestion that an extra charge at residue 283 is influential in the strength of the head-to-tail interaction, and that the strengthened head-to-tail interaction of phosphorylated Tm may be largely, if not solely, due to the negative charge associated to the phosphate group at residue 283.

Measurements of the Circular Dichroism Spectrum of Truncated Tropomyosin—For sedimentation equilibrium, the analysis is straight forward if the interaction between molecules is restricted to the dimeric type. Two types of Tm variants were therefore designed (Table I), one with a defective N-terminus and intact C-terminus and the other with an intact N-terminus and a defective C-terminus. By mixing these two species, only dimers are formed, multiple head-to-tail interactions being avoided.

It was then necessary to find suitable solution conditions for sedimentation equilibrium experiments. The criteria were maintaining (i) the α-helical structure of Tm and (ii) the head-to-tail interaction, and (iii) reducing non-specific interactions between molecules. At high ionic strengths, the strength of the head-to-tail interaction is reduced, whereas at low ionic strengths folding of the α-helical structure, especially at the C-terminus, is lost (*30*). The α-helical contents of the species were measured by circular dichroism and the head-to-tail interaction as well as non-specific interactions were identified in the protein density profiles resulting from the sedimentation equilibrium itself (see below).

Figure 2A shows the circular dichroism spectra of the

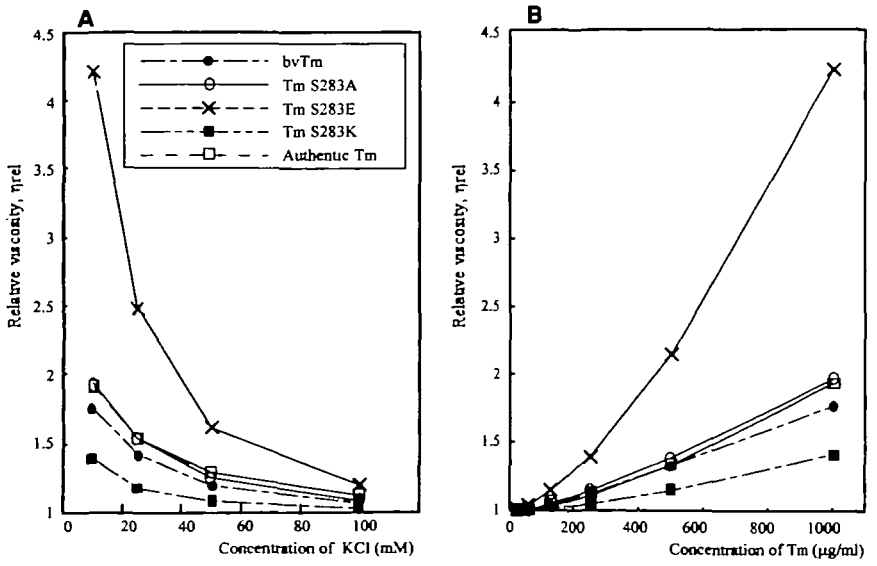

Fig. 1. **The relative viscosity of various serine-283 mutants of tropomyosin.** Filled circles, bvTm; open circles, Tm S283A; crosses, Tm S283E; filled squares, Tm S283K; open squares, dephosphorylated authentic Tm. A, the effect of ionic strength on the relative viscosity. The KCl concentration was varied from 10 to 100 mM with a fixed Tm concentration of 1 mg/ml. B, the effect of protein concentration. The concentration of Tm was varied from 25 μg/ml to 1 mg/ml with a fixed KCl concentration of 10 mM. The buffer conditions were 10 mM TrisHCl, pH 8.0, 0.5 mM DTT, and an appropriate concentration of KCl.

truncated Tm's at 10°C and Fig. 2B shows melting transition profiles of the truncated Tm's, both in 20 mM potassium phosphate buffer. Under these conditions, all three Tm species tested must assume the α-helical conformation. Thermal unfolding profiles indicated that the species including the C-terminal half, TmΔ1-140 and TmΔ1-140 S283E, were half unfolded at 33°C (Fig. 2B), which is substantially lower than the midpoint of the melting temperature curve at 47°C of the variant with truncation at the C-terminus, TmΔ274-284. The thermal unfolding profile of the latter also shows two transition steps. These results agree with those obtained from the corresponding fragments of Tm prepared by proteolytic digestion (*30*). At a lower ionic strength in 5 mM potassium phosphate buffer, the α-helical conformation is less stable; the unfolding profiles of TmΔ1-140 and TmΔ1-140 S283E shift to lower temperatures so that unfolding already occurs at 20°C, and the midpoint of the unfolding curves is at 26°C (data not shown). For these reasons, sedimentation equilibrium experiments were undertaken in 20 mM potassium phosphate buffer at 20°C.

Sedimentation Equilibrium—The association constant of the Tm head-to-tail interaction was measured directly using the sedimentation equilibrium method. Two pairs of Tm variants were used, each consisting of an N-terminal defective variant (either TmΔ1-140 or TmΔ1-140 S283E) and a C-terminal defective variant (TmΔ274-284). Neither variant exhibited self-association or non-ideal behavior when a single species was centrifuged (data not shown). Moreover, electronmicrographs of a rotary-shadowed mixture of the two species showed no multimer aggregates (data not shown). For these reasons, we assume that only three species were present in the Tm mixture: monomeric N-terminus defective variant, monomeric C-terminal defective variant, and the one-to-one complex of the two through head-to-tail interaction. Based on this assumption, the sedimentation equilibrium data were analyzed according to an ideal heterogeneously associating model: $A + B \leftrightarrow AB$ (*27*). In general, the sedimentation equilibrium method has potential for obtaining association constants in the range of 10^3–10^8 M^{-1} (*27*).

For the mixture of TmΔ274-284 and TmΔ1-140, when sedimentation equilibrium was attained, concentration gradient was formed in the cell as indicated in Fig. 3. The analysis of the gradients from 5 independent data sets yielded association constants between 0.8×10^4 and 3.5×10^4 M^{-1}, with an average 2.6×10^4 M^{-1} (SD = 1.0×10^4).

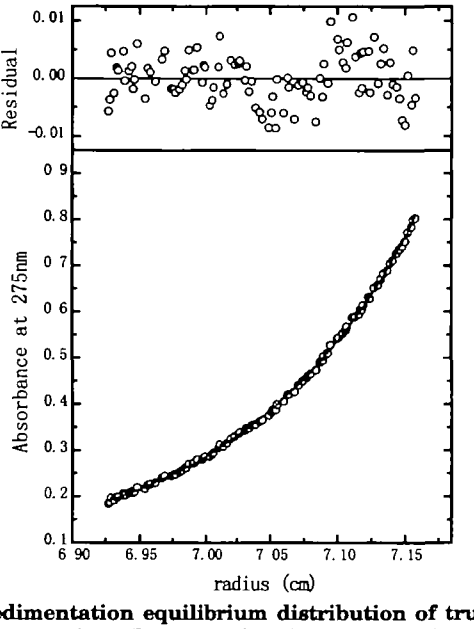

Fig. 3. **Sedimentation equilibrium distribution of truncated Tms concentrations (lower) and residuals (upper) as a function of the radial position of sector cells.** The protein solution contained 40 μM N-terminal truncated Tm (TmΔ1-140) and 20 μM C-terminal truncated Tm (TmΔ274-284) in 20 mM potassium phosphate buffer, pH 7.0, with 0.5 mM DTT. Centrifugation has been performed in an An-60Ti rotor on a Beckman Optima XL-A analytical ultracentrifuge at 12,000 rpm at 20°C. The data points were fitted by the continuous curve derived from Eq. 1 as explained in "MATERIALS AND METHODS". The residual was obtained as the difference between the fitted curve and the data point at each radial position.

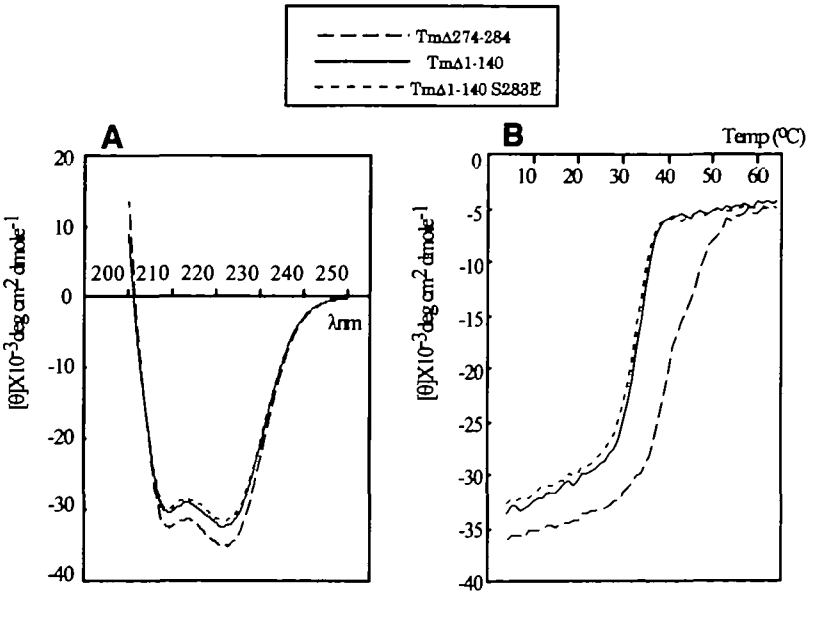

Fig. 2. **Circular dichroism spectra (A) and melting transition profiles (B) of truncated tropomyosin variants.** The broken lines are TmΔ274-284; the continuous lines are TmΔ1-140; the dotted lines are TmΔ1-140S283E. 5 μM (TmΔ274-284) or 10 μM (TmΔ1-140 and TmΔ1-140 S283E) truncated Tms in 20 mM potassium phosphate buffer, pH 7.0, and 0.5 mM DTT.

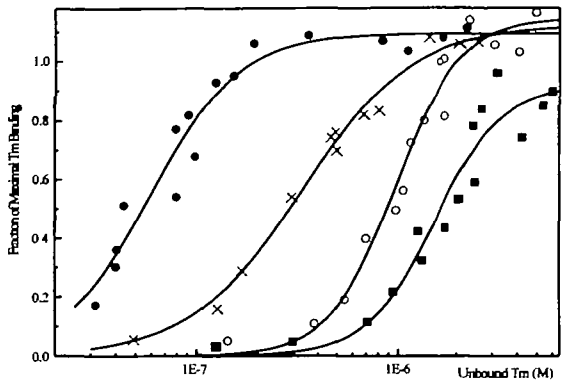

Fig. 4. **Actin binding properties of various tropomyosin serine-283 variants.** Fitted curves were drawn using the Hill equation (see "MATERIALS AND METHODS"). For each Tm variant, two to three independent sedimentation assays with F-actin were performed and the pooled data points are shown. Tm variants at 0.2–8 μM were cosedimented with 21 μM actin at room temperature in buffer containing 13 mM HEPES-NaOH, pH 7.0, 60 mM NaCl, 3 mM $MgCl_2$, 0.5 mM DTT, and 1 mM NaN_3. The symbols are the same as those used in Fig. 1.

We assume that the obtained value corresponds to the association constant of the head-to-tail interaction of the non-phosphorylated authentic rabbit skeletal Tm. This value is consistent with the previous estimation obtained by the light scattering measurements, 1.2×10^4 M^{-1} at 100 mM KCl (*18*). On the other hand, the association constants for TmΔ274-284 and TmΔ1-140 S283E were between 1.8×10^4 and 7.2×10^4 M^{-1} from 7 data sets, with an average 3.9×10^4 M^{-1} (SD = 1.6×10^4). This likely represents the association constant of the head-to-tail interaction of Tm phosphorylated at serine-283. The results indicate that, regardless of the amino acid at residue 283, the affinity of the head-to-tail interaction between adjacent tropomyosin molecules is weak. Moreover, the sedimentation equilibrium experiments apparently support the results of viscometry that an extra negative charge at residue 283 slightly strengthens the head-to-tail interaction, although the difference between the two variants is less significant as determined by sedimentation equilibrium ($p < 0.18$, Student's two-tailed *t*-test) than by viscometry.

Actin Binding of Tropomyosin Variants—The actin affinities of the Tm variants were measured by cosedimentation (Fig. 4 and Table II). The binding isotherms shown in Fig. 4 indicate that the pooled data points obtained from two or three independent experiments for each Tm variant fit Hill's equation to obtain an apparent binding constant (K_{app}) and Hill coefficient (α_H), which are summarized in Table II. Since bvTm is known to be identical to the authentic Tm in actin affinity (*19*, *29*), bvTm is used in the present study as the control. Since the phosphorylation of serine-283 did not alter the actin affinity (*12*), we had anticipated that the actin affinity of Tm S283E might not differ from that of bvTm. However, Tm S283E showed substantially lower actin affinity than bvTm. Tm S283A and Tm S283K bind actin even more weakly than Tm S283E. Interestingly, not only the apparent binding constant but also the parameter of cooperativity, α_H, differ clearly between species. As indicated in Table II, the α_H for Tm S283E is significantly smaller than those for Tm S283A and Tm S283K. Due to the strong affinity of bvTm, the data points at the lowest concentrations of free bvTm are missing making the α_H for this species somewhat unreliable. The data points in the region of higher concentrations of free Tm S283K are also scattered. The level of saturation for this species might be different from that of other species.

TABLE II. **Actin binding constants and Hill coefficients of tropomyosins.** The data shown in the binding isotherms in Fig. 2 were fit to the Hill equation ($v = n[Tm]^{\alpha_H}K_{app}^{\alpha_H}/1 + [Tm]^{\alpha_H}K_{app}^{\alpha_H}$, K_{app}, apparent binding constant; α_H, Hill coefficient). Data are reported as K_{app} and Hill coefficient ± SE calculated using MicroCal Origin™.

Tropomyosins	K_{app} (M^{-1})	Hill coefficient
bvTm	$1.7 \pm 0.1 \times 10^7$	2.0 ± 0.3
Tm S283A	$1.0 \pm 0.1 \times 10^6$	2.7 ± 0.4
Tm S283E	$3.0 \pm 0.2 \times 10^6$	1.6 ± 0.2
Tm S283K	$6.5 \pm 0.7 \times 10^5$	2.6 ± 0.6

DISCUSSION

The results presented here indicate that the strength of the head-to-tail interaction of tropomyosin molecules is substantially influenced by an extra charge at residue 283; an extra negative charge (as in Tm S283E and phosphorylated Tm) strengthens, whereas an extra positive charge (as in Tm S283K) weakens the head-to-tail interaction. On the other hand, the affinity of Tm to actin, as well as the cooperativity of actin binding, depends on amino acid residues in a more complicated manner. Tm S283E shows a lower affinity than phosphorylated Tm, although both species have an extra negative charge at 283. Tm S283E binds to actin in a less cooperative manner than Tm S283K or Tm S283A. These results suggest that the interaction with actin, the affinity and the cooperativity in actin binding, of skeletal muscle α-Tm is dependent on many factors including the stereoscopic occupancies of side chains at residue 283, and therefore these parameters are not simply correlated with the strength of the head-to-tail interaction between Tm molecules in solution.

After the experiments in the present study were completed, a positive correlation between the strength of the head-to-tail interaction and the cooperative activation of actomyosin subfragment 1 ATPase was reported (*31*). By undertaking comparative studies using rabbit skeletal muscle Tm (RSTm), chicken gizzard muscle Tm (GTm), and non-muscle Tm from rat fibroblast cells (5aTm), the authors interpreted the results to indicate that the higher cooperativity in the activation of ATPase is related to the GTm type of the C-terminal sequence shared by GTm and 5aTm but not by RSTm. They suggested that the sequence, therefore the structure, of the C-terminus should be a determining factor in the strength of the communication between adjacent Tm molecules on the actin filament, whereas the head-to-tail interaction of Tm alone, free from actin, should depend on both the N-terminus and C-terminus sequences. Their suggestion is consistent with our observations; there is no clear correlation between the strength of the head-to-tail interaction of Tm alone and the actin binding properties.

The present results indicate that the head-to-tail affinity between two Tm molecules in solution is weak. It may be

too weak and the difference in affinity may be too small to be a significant factor in cooperative actin binding. The cooperativity in actin binding must be governed by other factors, such as the manner of interaction between the C-terminus and actin molecules. It is worth noting that the difference in head-to-tail affinity as determined by sedimentation equilibrium measurement is much smaller than what would be expected from the large difference in viscosity, as is shown between two species of Tm with and without a negative charge at 283 (S283E versus the wild type with serine-283). This may be due to that fact that the viscosity is roughly in proportion to the square of the particle length, making the viscosity sensitive to the length of the Tm chains. It may be that our viscometry measurements did not pick up the elasticity of the Tm solution. Within the conditions employed in the present study, no effect of shear stress on the viscosity measurements was observed; the measured viscosity was not dependent on the number of measurements previously undertaken in the same viscometer.

In the present study, the association constant between two tropomyosin molecules through the head-to-tail interaction has been measured directly for the first time. For this purpose, sedimentation equilibrium measurements were employed with two pairs of truncated Tm variants, one between TmΔ274-284 and TmΔ1-140, and the other between TmΔ274-284 and TmΔ1-140 S283E. Truncated variants had to be used in order to prevent the formation of contiguous polymers that makes the analysis extremely complicated and ambiguous. Because these were variants, the possibility can not be excluded that the association constants obtained differ from those of the authentic molecule. We suggest, however, that these values are likely to be correct. First, as indicated in Fig. 2, the measurements were undertaken with the molecules in the coiled-coil configuration as the authentic molecules. Second, care was taken to reject any molecular species that showed non-specific (either attractive or repulsive) interactions. In the present study, a repulsive interaction between molecules of the same species was observed full length Tm with an unacetylated N-terminus expressed in *E. coli*; the sedimentation equilibrium of this single species gave rise to an apparent molecular weight that decreased with increasing protein concentration (data not shown). This is indicative of a repulsive force between the molecules, which may also be responsible for the loss of polymerizability and actin affinity.

It is worth noting that the tropomyosin species used in the present study were carefully designed based on the following considerations. First, Sf9 cells with baculovirus based expression systems were used for expressing any variant that extended to the original N-terminus, because N-terminal acetylation is required for actin binding and the head-to-tail interaction of tropomyosin (*14*). As an alternative to molecules with an acetylated N-terminus, molecules with extra residues at the N-terminus have been proposed, which facilitate both actin binding and the head-to-tail interaction (*29*, *32*). In the present study, however, species with an extended N-terminus were not used because the extra residues likely alter the association constant of the head-to-tail interaction. Moreover, we found no serious technical problem in the expression and purification of large quantities of these Tm species at high purity using the baculovirus-based expression system. Second, in order to study the effect of substituting one amino acid residue on the physicochemical and physiological properties of tropomyosin, two or more species were used that differ from each other only by one residue. Comparative studies of the physico-chemical properties using naturally occurring Tm species that differ from each other in the number of residues, may give rise to results that are difficult to interpret. Tropomyosin, the α-helical coiled-coil spans over almost the entire length of the polypeptide chain, so that almost all the residues may be involved in either intra- or inter-molecular interactions. Therefore replacement of any single residue may have a substantial effect on the manner of interaction with each other as well as with other protein molecules. The present study actually demonstrates such multiple effects of single residue replacements of α-Tm molecules.

We would like to thank Dr. Hisaaki Taniguchi of Fujita Health University for mass spectrometry, Ms. Yumiko Saijo for the generous gift of authentic rabbit Tm, Dr. Tomoyoshi Kobayashi for helpful advice concerning the experiments and useful discussion, Drs. Yoshinori Fujiyoshi and Kenji Iwasaki for their help in instruction and EM photography.

REFERENCES

1. Ebashi, S. and Endo, M. (1968) Calcium ion and muscle contraction. *Prog. in Biophys. Mol. Biolo.* **18**, 125–183
2. Ohtsuki, I., Maruyama, K., and Ebashi, S. (1986) Regulatory and cytoskeletal proteins of vertebrate skeletal muscle. *Adv. Protein Chem.* **38**, 1–67
3. Hitchcock-DeGregori, S.E. (1994) Structural requirements of tropomyosin for binding to filamentous actin. *Adv. Exp. Med. Biol.* **358**, 85–96
4. Pittenger, M.F., Kazzaz, J.A., and Helfman, D.M. (1994) Functional properties of non-muscle tropomyosin isoforms. *Curr. Opin. Cell. Biol.* **6**, 96–104
5. Kay, C. and Bailey, K. (1960) Light scattering in solutions of native and guanidinated rabbit tropomyosin. *Biochim. Biophys. Acta* **40**, 149–156
6. McLachlan, A.D. and Stewart, M. (1975) Tropomyosin coiled-coil interactions: evidence for an unstaggered structure. *J. Mol. Biol.* **98**, 293–304
7. Ebashi, S. (1972) Calcium ions and muscle contraction. *Nature* **240**, 217–218
8. Wegner, A. (1979) Equilibrium of the actin-tropomyosin interaction. *J. Mol. Biol.* **131**, 839–853
9. Walsh, T.P. and Wegner, A. (1980) Effect of the state of oxidation of cysteine 190 of tropomyosin on the assembly of the actin-tropomyosin complex. *Biochim. Biophys. Acta* **626**, 79–87
10. Wegner, A. (1980) The interaction of α, α- and α, β-tropomyosin with actin filaments. *FEBS Lett.* **119**, 245–248
11. Ribulow, H. and Barany, M. (1977) Phosphorylation of tropomyosin in live frog muscle. *Arch. Biochem. Biophys.* **179**, 718–720
12. Heeley, D.H., Watson, M.H., Mak, A.S., Dubord, P., and Smillie, L.B. (1989) Effect of phosphorylation on the interaction and functional properties of rabbit striated muscle alpha alpha-tropomyosin. *J. Biol. Chem.* **264**, 2424–2430
13. Johnson, P. and Smillie, L.B. (1977) Polymerizability of rabbit skeletal tropomyosin: effects of enzymic and chemical modifications. *Biochemistry* **16**, 2264–2269
14. Hitchcock-DeGregori, S.E. and Heald, R.W. (1987) Altered actin and troponin binding of amino-terminal variants of chicken striated muscle α-tropomyosin expressed in Escherichia coli. *J. Biol. Chem.* **262**, 9730–9735
15. Cho, Y.J. and Hitchcock-DeGregori, S.E. (1991) Relationship between alternatively spliced exons and functional domains in tropomyosin. *Proc. Natl. Acad. Sci. USA* **88**, 10153–10157
16. Hammell, R.L. and Hitchcock-DeGregori, S.E. (1996) Mapping

the functional domains within the carboxyl terminus of α-tropomyosin encoded by the alternatively spliced ninth exon. *J. Biol. Chem.* **271**, 4236–4242
17. Broschat, K.O. and Burgess, D.R. (1986) Low Mr tropomyosin isoforms from chicken brain and intestinal epithelium have distinct actin-binding properties. *J. Biol. Chem.* **261**, 13350–13359
18. Ooi, T., Mihashi, K., and Kobayashi, H. (1962) On the polymerization of tropomyosin. *Arch. Biochem. Biophys.* **98**, 1–11
19. Kluwe, L., Maeda, K., Miegel, A., Fujita-Becker, S., Maéda, Y., Talbo, G., Houthaeve, T., and Kellner, R. (1995) Rabbit skeletal muscle αα-tropomyosin expressed in baculovirus- infected insect cells possesses the authentic N-terminus structure and functions. *J Muscle Res. Cell. Motil.* **16**, 103–110
20. Studier, F.W., Rosenberg, A.H., Dunn, J.J., and Dubendorf, J.W. (1990) Use of T7RNA polymeriase to direct expression of cloned genes in *Methods in Enzymology*, Vol. 185, pp. 60–89, Academic Press, San Diego
21. O'Reilly, D.R., Miller, L.K., and Luckow, V.A. (1992) *Baculovirus Expression Vectors: A Laboratory Manual*, W.H. Freeman, New York
22. Sambrook, J., Fritsch, E.F., and Maniatis, T. (1989) *Molecular Cloning: A Laboratory Manual*, 2nd ed., Cold Spring Harbor Laboratory, Cold Spring Harbor, NY
23. Miegel, A., Sano, K.I., Yamamoto, K., Maeda, K., Maéda, Y., Taniguchi, H., Yao, M., and Wakatsuki, S. (1996) Production and crystallization of lobster muscle tropomyosin expressed in Sf9 cells. *FEBS Lett.* **394**, 201–205
24. Suzuki, N. and Mihashi, K. (1991) Binding mode of cytochalasin B to F-actin is altered by lateral binding of regulatory proteins. *J. Biochem.* **109**, 19–23
25. Smillie, L.B., Pato, M.D., Pearlstone, J.R., and Mak, A.S. (1980) Periodicity of α-helical potential in tropomyosin sequence correlates with alternating actin binding sites. *J. Mol. Biol.* **136**, 199–202
26. Takeda, S., Kobayashi, T., Taniguchi, H., Hayashi, H., and Maeda, Y. (1997) Structural and functional domains of the troponin complex revealed by limited digestion. *Eur. J. Biochem.* **246**, 611–617
27. Hensley, P. (1996) Defining the structure and stability of macromolecular assemblies in solution: the re-emergence of analytical ultracentrifugation as a practical tool. *Structure* **4**, 367–373
28. Tanford, C. (1961) *Physical Chemistry of Macromolecules*, John Wiley & Sons, New York
29. Urbancikova, M. and Hitchcock-DeGregori, S.E. (1994) Requirement of amino-terminal modification for striated muscle α-tropomyosin function. *J. Biol. Chem.* **269**, 24310–24315
30. Pato, M.D., Mak, A.S., and Smillie, L.B. (1981) Fragments of rabbit striated muscle α-tropomyosin. I. Preparation and characterization. *J. Biol. Chem.* **256**, 593–601
31. Lehrer, S.S., Golitsina, N.L., and Geeves, M.A. (1997) Actin-tropomyosin activation of myosin subfragment 1 ATPase and thin filament cooperativity. The role of tropomyosin flexibility and end-to-end interactions. *Biochemistry* **36**, 13449–13454
32. Monteiro, P.B., Lataro, R.C., Ferro, J.A., and Reinach, F.d.C. (1994) Functional α-tropomyosin produced in Escherichia coli. A dipeptide extension can substitute the amino-terminal acetyl group. *J. Biol. Chem.* **269**, 10461–10466